Calmodulin Modulates Initiation but Not Termination of Spontaneous Ca^{2+} Sparks in Frog Skeletal Muscle

George G. Rodney and Martin F. Schneider
Department of Biochemistry and Molecular Biology, University of Maryland School of Medicine, Baltimore, Maryland 21201

ABSTRACT Calmodulin is a ubiquitous Ca^{2+} sensing protein that binds to and modulates the sarcoplasmic reticulum Ca^{2+} release channel, ryanodine receptor (RYR). Here we assessed the effects of calmodulin on the local Ca^{2+} release properties of RYR in permeabilized frog skeletal muscle fibers. Fluorescently labeled recombinant calmodulin in the internal solution localized at the Z-line/triad region. Calmodulin (0.05–5.0 μM) in the internal solution (free $[Ca^{2+}]_i$ ~50–100 nM) initiated a highly cooperative dose-dependent increase in Ca^{2+} spark frequency, with a half-maximal activation (K) of 1.1 μM, a Hill coefficient (n) of 4.2 and a fractional maximal increase in frequency (R) of 17-fold. A non-Ca^{2+} binding mutant of calmodulin elicited a similar highly cooperative dose-dependent increase in spark frequency ($K = 1.0$ μM; $n = 3.7$; $R = 12$-fold). Spatiotemporal properties of Ca^{2+} sparks were essentially unaffected by either wild-type or mutant calmodulin. An N-terminal extension of calmodulin, (N+3)calmodulin, that binds to but does not activate RYR at nM $[Ca^{2+}]$ in sarcoplasmic reticulum vesicles, prevented the calmodulin-induced increase in spark frequency. These data suggest that exogenous Ca^{2+}-free calmodulin cooperatively sensitizes the Ca^{2+} release channel to open, but that Ca^{2+} binding to the added calmodulin does not play a significant role in the termination of Ca^{2+} sparks.

INTRODUCTION

Many accessory molecules can modulate the function of the sarcoplasmic reticulum Ca^{2+} release channel, ryanodine receptor (RYR). These include small molecules such as Ca^{2+}, Mg^{2+}, hydrogen ion, adenine nucleotides, oxidants, nitric oxide, ryanodine, caffeine, ruthenium red, as well as regulatory proteins such as FK-506 binding protein (FKBP12), junctin, triadin, calsequestrin and calmodulin (CaM) (for review see Fill and Copello, 2002; Ogawa et al., 2002).

Calmodulin (CaM) is a highly conserved Ca^{2+} binding protein that plays a central role in Ca^{2+} signaling in eukaryotic cells (James et al., 1995). CaM is a 148 amino acid (~17 kDa), very acidic (pI ~4.0), heat stable protein. The amino acid sequence of CaM is highly conserved among a diverse number of species, including slime mold, unicellular alga, *Drosophila*, yeast, and mammals. The highly conserved amino acid sequence of CaM reflects the importance of CaM as a transducer of the Ca^{2+} signal. CaM contains two globular domains each consisting of two EF-hand Ca^{2+} binding pockets. The four Ca^{2+} binding sites of CaM have a relatively high affinity for Ca^{2+}. The binding of Ca^{2+} to CaM exposes hydrophobic patches on the surface of CaM, allowing it to bind to a variety of target proteins. Although CaM requires Ca^{2+} (Ca^{2+}CaM) for binding and activation of many of its target proteins, there are an increasing number of proteins that bind Ca^{2+}-free CaM, including the sarcoplasmic reticulum (SR) Ca^{2+} release channel, RYR (Moore et al., 1999; Rodney et al., 2000; Tripathy et al., 1995; Yamaguchi et al., 2001), and the α_{1s} subunit of the voltage dependent Ca^{2+} channel, dihydropyridine receptor (DHPR) (Pate et al., 2000; Sencer et al., 2001).

Each ryanodine receptor type-1 (RYR1) subunit binds one molecule of CaM at both nM and μM Ca^{2+} concentrations, or four CaM molecules per RYR1 tetramer (Moore et al., 1999). Despite binding the same number of CaM molecules at nM and μM Ca^{2+} concentrations, CaM displays Ca^{2+} dependence in its functional effects on RYR1. At nM Ca^{2+} concentrations Ca^{2+}-free CaM activates RYR1 while at μM Ca^{2+} concentrations Ca^{2+}CaM inhibits RYR1 (Rodney et al., 2000). Furthermore, using a mutant CaM that cannot bind Ca^{2+} (CaM_{1234}) these authors have shown that Ca^{2+} binding to CaM converts CaM from an activator to an inhibitor of RYR1. These studies suggest that CaM does not simply sensitize RYR1 to Ca^{2+} but that CaM senses changes in $[Ca^{2+}]_i$, transducing these changes into functional alterations of RYR1. It is therefore conceivable that CaM may play an important role in activation and/or termination of Ca^{2+} release from the SR in skeletal muscle.

In muscle RYR activity gives rise to localized, discrete elevations in myoplasmic $[Ca^{2+}]$, Ca^{2+} ''sparks'' (Cheng et al., 1993; Klein et al., 1996). The measurement of Ca^{2+} sparks provides a good way to assess the function and regulation of RYR in a quasiphysiological setting. Ca^{2+} sparks have been measured in frog skeletal muscle upon fiber depolarization as well as ''spontaneously'' in the absence of voltage sensor activation (Klein et al., 1996). These authors showed that the frequency of discrete Ca^{2+} release events increased steeply with increasing fiber depolarization, suggesting that Ca^{2+} sparks underlie the macroscopic Ca^{2+} transient. Spontaneous Ca^{2+} sparks are initiated by ligand activation and are terminated by inactivation of RYR, independent of voltage sensor activation. Activation and

Submitted January 29, 2003, and accepted for publication April 3, 2003.

Address correspondence to M. F. Schneider, Dept. of Biochemistry and Molecular Biology, University of Maryland School of Medicine, 108 N. Greene St., Baltimore, MD 21201. Tel.: 410-706-7812; Fax: 410-706-8297; E-mail: mschneid@umaryland.edu.

0006-3495/03/08/921/12 $2.00

termination of Ca^{2+} release during a Ca^{2+} spark occurs abruptly (Lacampagne et al., 1999). An increase in myoplasmic [Ca^{2+}] (Klein et al., 1996) and a decrease in myoplasmic [Mg^{2+}] (Lacampagne et al., 1998) increases the frequency of occurrence of spontaneous Ca^{2+} sparks, consistent with a model of Ca^{2+} induced Ca^{2+} release (CICR). The inactivation of spontaneous Ca^{2+} sparks is less understood. Lacampagne et al. (1998) have shown that the kinetics of Ca^{2+} spark termination are independent of myoplasmic [Mg^{2+}] and thus the closing of channels is by some other mechanism than Mg^{2+} binding to inhibitory sites on the channel. One possibility might be Ca^{2+}CaM dependent inactivation of the channels.

In this study we have used recombinant CaMs to determine whether CaM can modulate the microscopic Ca^{2+} release events in frog skeletal muscle fibers permeabilized by brief exposure to saponin. Although saponin permeabilized fibers may not completely reproduce all conditions in an intact fiber, they should maintain many of the macromolecular interactions of intact fibers, and provide a very convenient method to apply variable concentrations of exogenous proteins to the interior of a muscle fiber. Here we find that exogenously applied CaM localizes to the triad and causes a highly cooperative dose-dependent increase in Ca^{2+} spark frequency. Neither wild-type CaM nor CaM_{1234} induced a physiologically meaningful alteration in the spatial or temporal properties of Ca^{2+} sparks. Our data suggest that CaM acts to promote activation of RYR but that termination of Ca^{2+} sparks may be through a Ca^{2+}CaM independent mechanism.

MATERIALS AND METHODS

Expression and purification of calmodulin

The cDNA for CaM, and CaM_{1234} and the protein (N+3)CaM have been graciously provided by Dr. Susan L. Hamilton (Baylor College of Medicine, Houston, TX). cDNAs were confirmed by sequence analysis. For expression, BL21-DE3 *E. coli* transformed with the pET3-CaM or pET3-CaM_{1234} plasmid was induced with 0.3 mM β-D-thiogalactopyranoside (IPTG) for 4 h at 37°C. Expressed CaMs were purified as previously described (Rodney et al., 2000). Purity of each CaM was assessed by SDS-PAGE and protein concentration was determined by measuring the absorbance (A) at 277 and 320 nm and calculating the concentration (C) according to Eq. 1 (Richman and Klee, 1979),

$$C = (A_{277} - A_{320})/\varepsilon, \quad (1)$$

where $\varepsilon = 1874\ \mathrm{L\ M^{-1}\ cm^{-1}}$ for CaM and $1900\ \mathrm{L\ M^{-1}\ cm^{-1}}$ for CaM_{1234} in 1 mM ethylene glycol-bis(β-aminoethylether)-N,N,N',N'-tetraacetic acid (EGTA) (Mukherjea et al., 1996). Purified recombinant CaM was labeled with Alexa Fluor 488 (Molecular Probes, Eugene OR) using the Alexa Fluor 488 protein labeling kit according to manufacturer's instructions.

Preparation of skeletal muscle fibers

Frogs (*Rana pipiens*) were first placed in a cold-induced torpor (crushed ice-water slurry, 20 min) followed by rapid decapitation and spinal cord destruction according to protocols approved by the University of Maryland Institutional Animal Care and Use Committee. The ileofibularis muscle was removed and pinned in a dissecting chamber containing Ringer's solution (in mM): 115 NaCl, 2.5 KCl, 1.8 $CaCl_2$, 1.0 $MgCl_2$, 10 HEPES, pH 7.0. Small fiber segments (3–5 mm) were manually disected in relaxing solution containing (mM): 120 k-glutamate, 2 $MgCl_2$, 1 EGTA, 5 Na-tris-maleute, pH 7.00 and mounted in an experimental chamber (3.8 ± 0.4 μm per sarcomere) containing relaxing solution as previously described (Lacampagne et al., 1998). Bathing the fiber in a relaxing solution containing 0.01% saponin and 1.0 mM EGTA for 30–40 s chemically permeabilized fibers, allowing for solution equilibration into the myoplasm. Immediately following the permeabilization procedure, the fiber was bathed in internal solution containing (in mM) 80 K-glutamate, 5.5 $MgCl_2$, 5 Na_2ATP, 20 tris-maleate, 0.1 EGTA, 20 Na_2-creatine phosphate, 5 glucose, 0.05 Fluo-3 (pentapotassium salt) (Molecular Probes, Eugene, OR), pH 7.0 supplemented with 8% Dextran (41 kD). Dextran was utilized to avoid the osmotic swelling seen in chemically permeabilized fibers (Tsuchiya, 1988; Ward et al., 1998). CaM and mutant CaMs were added to the internal solution from stock solutions. A complete change of the bathing solution occurred upon the addition of CaM and fibers were allowed to equilibrate for 10 min prior to data collection. To control for bath solution change and time ''sham'' fibers were exposed to the same conditions as those fibers in the CaM group except that CaM was not added to the internal solution.

Localization of recombinant CaM

For localization of recombinant CaM saponin permeabilized fibers were incubated with CaM-488 (1 μM) and either BODIPY TR-X ryanodine (10 nM, Molecular Probes, Eugene OR), or Texas Red-X phalloidin (775 nM, Molecular Probes, Eugene OR) for 20 min in internal solution. Fibers were then washed with internal solution prior to image acquisition. In competition studies saponin permeabilized fibers were incubated with (N+3)CaM (2 μM) for 10 min in internal solution. The solution was then changed to an internal solution containing CaM-488 (1 μM) plus (N+3)CaM (2 μM) and allowed to incubate for 20 min. The bath was then changed to internal solution alone prior to image acquisition.

Immunofluorescence labeling of endogenous CaM

Single ileofibularis muscle fibers were dissected and mounted in the experimentsl chamber in relaxing solution, fixed with 4% paraformaldehyde in PBS, washed three times with PBS followed by permeabilization for 10 min with 0.1% triton in PBS. Fibers were washed 3 times with PBS and stored at 4°C until used for immunohistochemistry. To determine if endogenous CaM levels are altered by our saponin permeabilization a group of fibers were permeabilized and treated exactly the same as for Ca^{2+} spark analysis (i.e., internal solution except with no Fluo-3 dye for 10 min) prior to paraformaldehyde fixation, followed by the subsequent steps described above. Fibers were stained overnight at 4°C with a monoclonal primary antibody against CaM (Mouse anti-calmodulin, Zymed Laboratories Inc., South San Francisco, CA). Primary antibody labeling was followed by labeling with a FITC conjugated goat anti-mouse secondary antibody (Jackson ImmunoResearch, West Grove, PA).

Confocal fluorescence measurements

For localization of CaM-488 and either BODIPY TR-X ryanodine or Texas Red-X phalloidin, confocal fluorescent x-y images were taken on a Bio-Rad Radiance 2100 scanning confocal system coupled to an inverted microscope (Olympus IX-70 with an Olympus 60×, 1.2 NA water immersion objective). The optical resolution of the system was 0.32 μm in the x and y dimension and 0.6 μm in the z dimension as determined using 0.1 μm fluorescence beads in air. For immunofluorescence labeling of CaM and for Ca^{2+} spark measurements fiber fluorescence was measured using a laser scanning confocal system (Bio-Rad MRC 600) coupled to an inverted microscope (Olympus IX-

70 with an Olympus 60×, 1.4 NA oil immersion objective). Immunofluorescence images were acquired in *x-y* mode. For Ca^{2+} spark studies the confocal system was operated in linescan *x-t* mode (1024 ms acquisition time, 2 ms per line, 768 pixels per line, 0.18 μm per pixel). The confocal aperture was set to 25% of the maximal value, in which the resolution was estimated as 0.4 μm in the *x* and *y* dimensions, and 0.8 μm in the *z* dimension as determined using 0.1 μm fluorescence beads in air. Each linescan run consisted of five images acquired at the same line location (e.g., a total of 5 s of acquisition). To avoid photodynamic damage of the fiber, the laser intensity was set to the minimal power giving a reasonable fluorescence intensity, and acquisition during successive runs was performed by moving the scanned line position by 0.9 μm perpendicular to the fiber long axis between runs.

In each set of linescan images regions of interest (ROI) in which potential Ca^{2+} sparks occurred were detected by an automatic computer detection algorithm as previously described (Shtifman et al., 2000) as modified from Cheng et al. (1999). Images were corrected for PMT offset then converted to ΔF by subtraction of the spatial (*x*) pattern of resting fluorescence (F) along the fiber averaged in time over the entire duration of the five images, excluding the contribution of potential Ca^{2+} spark ROIs. ΔF images were then normalized pixel by pixel by F and smoothed 3 × 3 to give the $\Delta F/F$ images. Temporal profiles were extracted from each ROI as the mean of three spatial pixels centered at the peak $\Delta F/F$ and fit to a sequence of two exponentials functions (Lacampagne et al., 1999). Spatial information was determined from a mean of three temporal pixels centered at the peak $\Delta F/F$ within the ROI and fit to a Gaussian function. For each selected event, the peak amplitude, rise time, temporal half-duration (full duration at half-max; FDHM) and spatial half-width (full width at half-max; FWHM) were determined from the temporal and spatial fits. Events with a $\Delta F/F < 0.4$ were excluded from data analysis post-hoc. The frequency of events per sarcomere was calculated from the number of sparks per image divided by the number of sarcomeres along the line and by the image duration (1.024 s).

Data analysis

Ca^{2+} spark frequency results are reported as means ± SE. To account for the variability in the starting Ca^{2+} spark frequency amongst fibers each data point was normalized to the average Ca^{2+} spark frequency for the same group of fibers prior to the addition of exogenous protein. Statistical analysis for comparison of means was performed using analysis of variance (ANOVA) with a significance level of $P < 0.05$. The spatiotemporal properties of Ca^{2+} sparks (amplitude, rise time, FDHM, and FWHM) were not normally distributed, therefore a nonparametric ANOVA was performed (Dunn's). All statistical analysis was performed with SigmaStat and nonlinear curve fitting was performed in SigmaPlot (Jandel).

RESULTS

Recombinant calmodulin localizes to the triad in skeletal muscle

Saponin permeabilization has been used to provide access to the internal environment of skeletal muscle, permitting fluorescent dyes, large molecules and small peptides to enter the cell (Gonzalez et al., 2000; Shtifman et al., 2000; Shtifman et al., 2001). To ensure that recombinant CaM can gain access to the myoplasm we investigated the localization of Alexa Fluor 488 labeled CaM (CaM-488) in saponin permeabilized muscle fibers. Fig. 1 shows that CaM-488 displayed a single predominant band in a sarcomeric pattern (Fig. 1, *A* and *E*). To determine the sarcomere localization of this pattern, simultaneous labeling with CaM-488 and either BODIPY TR-X ryanodine (Fig. 1, *B* and *C*) or Texas Red phalloidin (Fig. 1, *F* and *G*) was investigated. BODIPY TR-X ryanodine displayed a single sharp band at each sarcomere (Fig. 1 *B*) and most CaM-488 colocalized with TR-X ryanodine (Fig. 1, *C* and *D*), presumably at the single triad per sarcomere at the Z-line in frog skeletal muscle. A faint CaM-488 line midway between Z-lines (Fig. 10) indicates weaker binding at the M-line region. The localization pattern of CaM-488 observed here in frog skeletal muscle fibers is consistent with a previous study, which showed CaM localizing predominantly to the Z-line with some staining at the M-line in mammalian skeletal muscle (Harper et al., 1980). The Texas Red phalloidin fluorescent pattern showed a characteristic broader triplet, where the bright center peak corresponding to the Z-line and the two less fluorescence shoulders on either side of the bright peak stain the thin filaments (Bukatina et al., 1984) (Fig. 1, *F* and *H*). CaM-488 colocalized with the bright center peak of the phalloidin pattern (Fig. 1, *G* and *H*). To test the specificity of the CaM-488 pattern we used a non-fluorescent dominant-negative form of CaM, (N+3) CaM, and determined its ability to prevent the CaM-488 localization. (N+3)CaM has a three amino acid (Gly-Ser-His) extension at its N-terminus, resulting in a four- to fivefold higher affinity for RYR1 than wild-type CaM, but does not enhance [^{3}H]ryanodine binding to RYR1 under the $[Ca^{2+}]_i$ (50–100 nM) used in the current experiments (Xiong et al., 2002). Fig. 2 shows that the addition of (N+3) CaM (2 μM) prevented the sarcomeric localization of CaM-488 (1 μM). Taken together, these results indicate that exogenously added recombinant CaM localizes to the Z-line (i.e., the triad) in frog skeletal muscle, the precise area in which Ca^{2+} sparks originate (Klein et al., 1996).

Saponin permeabilization does not result in a loss of endogenous calmodulin

Immunofluorescence labeling for endogenous CaM in frog skeletal muscle showed a sarcomeric pattern, with a single fluorescent band per sarcomere (Fig. 3 *A*). To determine if brief saponin permeabilization of frog skeletal muscle results in an appreciable loss of endogenous CaM we immunolabeled skeletal muscle fibers that had been saponin permeabilized and bathed in internal solution for 10 min prior to fixation. Fig. 3 shows that our permeabilization protocol does not result in an appreciable loss of endogenous CaM. The average fiber fluorescence was 12.4 ± 0.6 fluorescence units (F.U.) in nonpermeabilized fibers (Fig. 3 *A*, $n = 5$) and 15.3 ± 0.6 F.U. in the permeabilized fibers (Fig. 3 *B*, $n = 5$). Fig. 3, *C* and *D*, shows that there is no detectable fluorescence in the presence of secondary antibody alone.

Effects of calmodulin on Ca^{2+} sparks

To investigate the role of CaM on localized Ca^{2+} release events we monitored the frequency and properties of Ca^{2+}

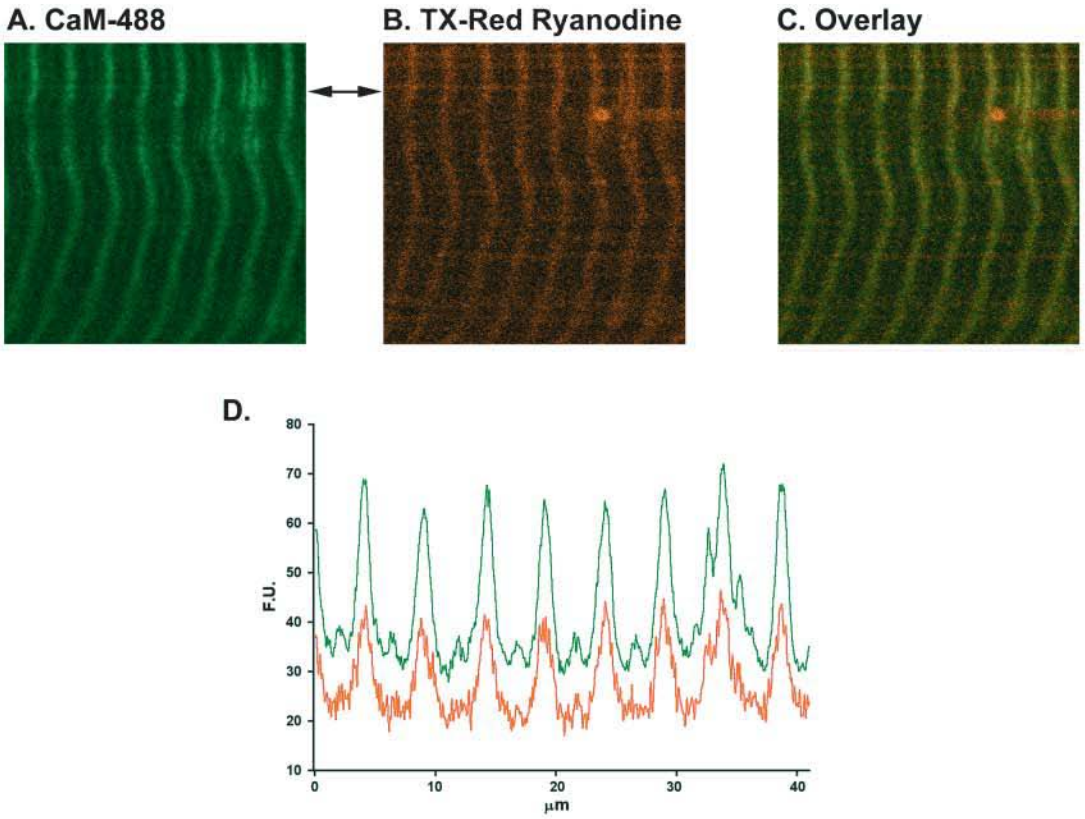
A. CaM-488
B. TX-Red Ryanodine
C. Overlay
D.
F.U.
μm
E. CaM-488
F. TX-Red Phalloidin
G. Overlay
5 μm
H.
F.U.
μm

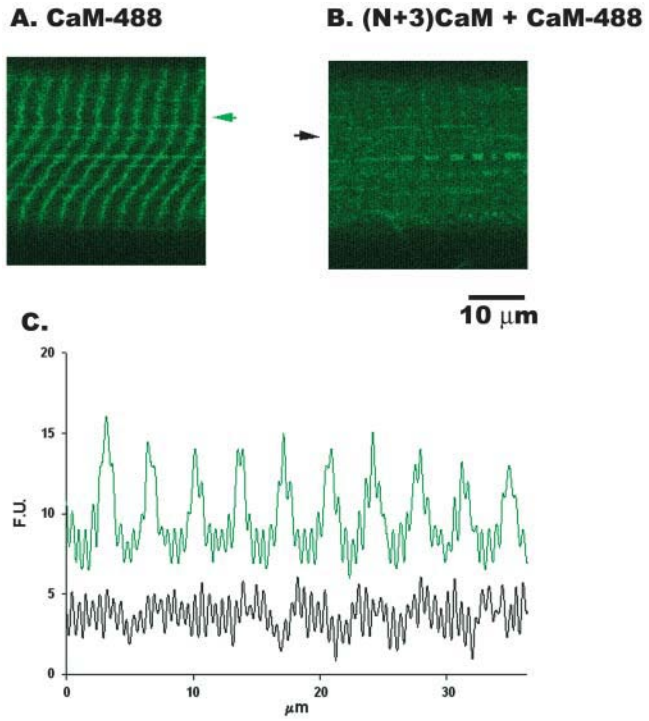

FIGURE 2 Effect of (N+3)CaM on CaM-488 localization. (N+3)CaM (2 μM, panel *B*) prevents the localization of CaM-488 (1 μM, panel *A*). Data in panels *A* and *B* are from different fibers. Panel *C* shows the line profile for the CaM-488 pattern from panel *A* (*green curve* and *arrow*) and from panel *B* (*black curve* and *arrow*).

sparks under control conditions, after addition of either CaM or the dominant-negative (N+3)CaM, or after a ''sham'' solution change with no added CaM. These studies were conducted under conditions in which the internal solution contained a free $[Mg^{2+}]_i$ of 0.65 mM, which provides a reasonably detectable control resting frequency of Ca^{2+} sparks, so that either an increase or a decrease in Ca^{2+} spark frequency could be observed (Lacampagne et al., 1998; Shtifman et al., 2001). Fig. 4 shows a representative line-scan fluorescence ($\Delta F/F$) image under control conditions (Fig. 4, *A* and *C*), after the addition of CaM (1 μM, Fig. 4 *B*) or after the addition of 1 μM CaM in the presence of (N+3)CaM (2 μM) (Fig. 4 *D*). Displayed below each image is the $\Delta F/F$ time course at a single triad in which a Ca^{2+} spark occurred. Addition of CaM (1 μM) resulted in an approximately ninefold increase in the frequency of Ca^{2+} sparks (Figs. 4 *B* and 5) whereas (N+3)CaM (1 μM) had no effect on Ca^{2+} spark frequency (Fig. 5). Furthermore,

FIGURE 1 Localization of CaM-488 in frog skeletal muscle. Saponin permeabilized frog skeletal muscle was stained with CaM-488 (*A* and *E*) and either BODIPY TR-X ryanodine (*B*) or Texas Red-X phalloidin (*F*). CaM-488 was found to colocalize with ryanodine (*C*) and the bright phalloidin band (*G*). Images *C* and *G* are color overlays of the images to the left. Panels *D* and *H* show the line profiles taken from panels *A* (*green curve*) and *B* (*red curve*) or panels *E* (*green curve*) and *F* (*red curve*), respectively, at the indicated positions (*arrow*).

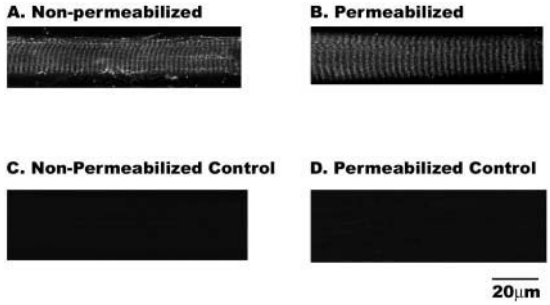

FIGURE 3 Immnufluorescence labeling of endogenous CaM in cut nonpermeabilized (*A*) or saponin permeabilized (*B*) frog skeletal muscle fibers. Panels *C* and *D* show that there is no detectable fluorescence from fibers incubated in secondary antibody alone.

addition of excess (N+3)CaM (2 μM) before and during application of CaM (1 μM) largely prevented the increase in Ca^{2+} spark frequency observed with CaM alone (Figs. 4 and 5). The frequency of Ca^{2+} sparks in the presence of 2 μM (N+3)CaM alone was not different than that observed at 1 μM (N+3)CaM (data not shown). Thus, addition of (N+3)CaM at these concentrations does not appear to eliminate any possible activating effect on Ca^{2+} spark frequency produced by any remaining endogenous CaM.

To determine whether the increase in Ca^{2+} spark frequency after adding CaM was associated with an alteration of the kinetics of the release event, we analyzed the spatiotemporal properties of individual Ca^{2+} release events. Fig. 6 represents histograms of the spatiotemporal properties and the corresponding median box plots for 1467 and 3120 Ca^{2+} release events ($\Delta F/F \geq 0.4$) after the sham solution change and after the addition of exogenous CaM (1 μM), respectively. Median values for the spatiotemporal properties in sham and CaM groups are reported in Table 1. Upon addition of CaM there was a small albeit statistically significant decrease in the amplitude (5.7%), and FWHM (5.1%). Rise time and FDHM were not significantly different between sham and CaM. Overall, the predominant effect of 1 μM CaM in permeabilized frog skeletal muscle was to markedly increase the frequency of spontaneous Ca^{2+} sparks, with at most only very minor changes in spark properties.

Calmodulin displays cooperativity in its enhancement of Ca^{2+} spark activity

We next assessed the relationship between the increase in Ca^{2+} spark frequency and the concentration of added CaM. CaM (0.05–5.0 μM) elicited a nonlinear, dose-dependent, saturating increase in Ca^{2+} spark frequency (Fig. 7 *A*). The solid line was obtained by fitting the data to the following equation:

$$f = f_{min}(R-1)(x^n/(K^n + x^n)) + f_{min}, \quad (2)$$

where f is the event frequency normalized to the average event frequency in the same group of fibers prior to CaM

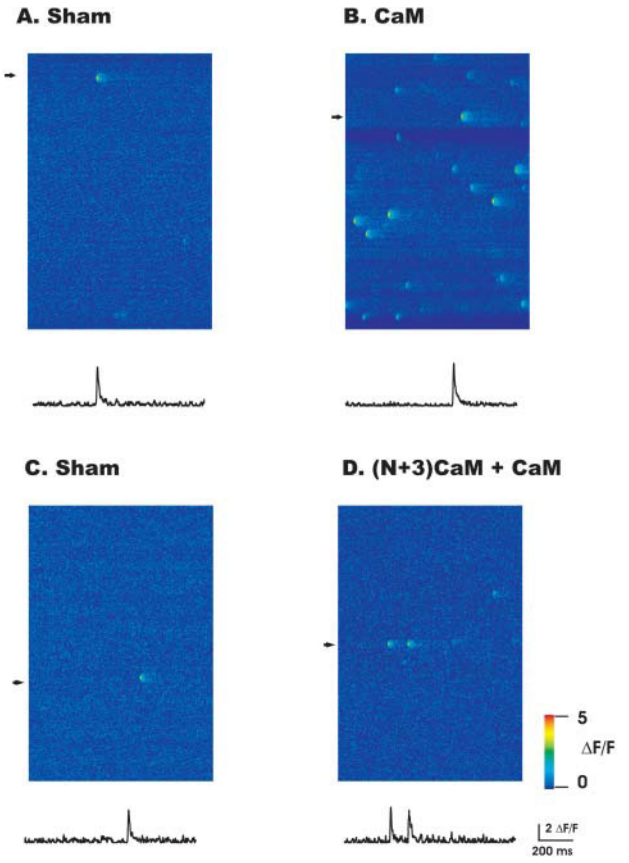

FIGURE 4 Representative linescan images (*top*) and temporal time courses (*bottom*) from permeabilized frog skeletal muscle. The temporal time courses represent the average of three spatial pixels centered at the fluorescence peak at the indicated individual triads (*arrow heads*) in the image. (*A* and *C*) Discrete localized Ca^{2+} sparks under control conditions. (*B*) CaM (1μM) increased the frequency of Ca^{2+} sparks but did not alter the spatial or temporal properties. (*D*) (N+3)CaM (2 μM) prevents the CaM-induced increase in Ca^{2+} spark frequency.

application, R is the fractional maximal increase (f_{max}/f_{min}), n is the Hill coefficient, and K is the concentration of CaM that elicits 50% of the increase in frequency (EC_{50}). Fit of the data using Eq. 2 gave a fractional maximal increase (R) of 17.3 $\pm$ 5.5, with a half-maximal activation of 1.1 $\pm$ 0.1 μM. A Hill coefficient of 4.2 $\pm$ 1.1 suggested high cooperativity in the CaM dependent initiation of Ca^{2+} sparks. In light of results showing low cooperativity in the CaM dependent enhancement of [^{3}H]ryanodine binding in SR vesicles (Tripathy et al., 1995), the high degree of cooperativity in the CaM dependence of Ca^{2+} spark frequency seen here in muscle fibers was unexpected and will be discussed in further detail (see Discussion). Analysis of the spatiotemporal properties of Ca^{2+} release events showed that amplitude, rise time, FDHM, and FWHM did not differ at these different CaM concentrations (data not shown).

Fig. 7 *B* shows the average fluorescence of linescan images in the presence of CaM normalized to F prior to CaM application for the same fibers and the same experiments as

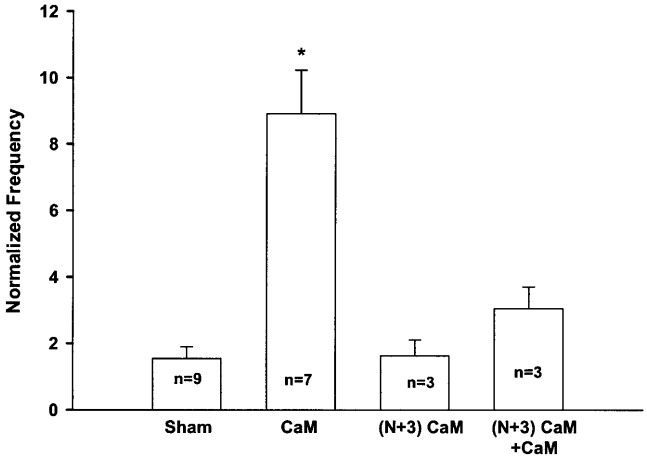

FIGURE 5 CaM increases spontaneous Ca^{2+} spark in permeabilized frog skeletal muscle. Frequency was determined as the mean number of events identified in each fiber and normalized to the mean frequency of that group of fibers prior to the addition of CaM (1 μM), (N+3)CaM (1 μM) or (N+3)CaM (2 μM) plus CaM (1 μM). The Sham condition describes the effect of buffer change without addition of CaM or (N+3)CaM, i.e., buffer control. Bars represent mean $\pm$ SE of the number of fibers indicated for each bar. *$P < 0.05$ versus all groups.

tested in Fig. 7 *A*. Potential location of Ca^{2+} sparks were excluded from the average fluorescence. No significant change in average fluorescence was observed, suggesting that the observed increase in Ca^{2+} spark frequency is not due to an elevation in resting [Ca^{2+}]. Furthermore, since the Ca^{2+} release events were measured in the presence of the added CaM (i.e., the CaM was not removed before recording) the fact that the average fluorescence as well as the spatiotemporal properties of the release events were not different at the tested CaM concentrations indicates that CaM is not significantly competing with the indicator dye for Ca^{2+}.

The saturating effect of CaM on Ca^{2+} spark frequency observed here was unlike previous observations of a linear relationship between Ca^{2+} spark frequency and modulator concentration (Lacampagne et al., 1998; Shtifman et al., 2000, 2001). To verify that the saturation of Ca^{2+} spark frequency observed with CaM was not due to a limitation of our ability to discern individual Ca^{2+} release events we assessed the effect of CaM (3 μM) on the occurrence of Ca^{2+} sparks under conditions of potentiated Ca^{2+} release (0.13 mM Mg^{2+}_{free}). Under low $[Mg^{2+}]_{free}$ conditions (0.13 mM) and 3 μM CaM the normalized Ca^{2+} spark frequency was 34.1 $\pm$ 1, a 63% increase compared to 3 μM CaM in 0.65 mM Mg^{2+}_{free}. Fig. 8 shows that discrete localized Ca^{2+} sparks can still be identified under these conditions.

Role of calmodulin in termination of the Ca^{2+} spark

Since CaM increases the open probability of RYR in single channel bilayer studies under nM [Ca^{2+}]$_i$ and since our

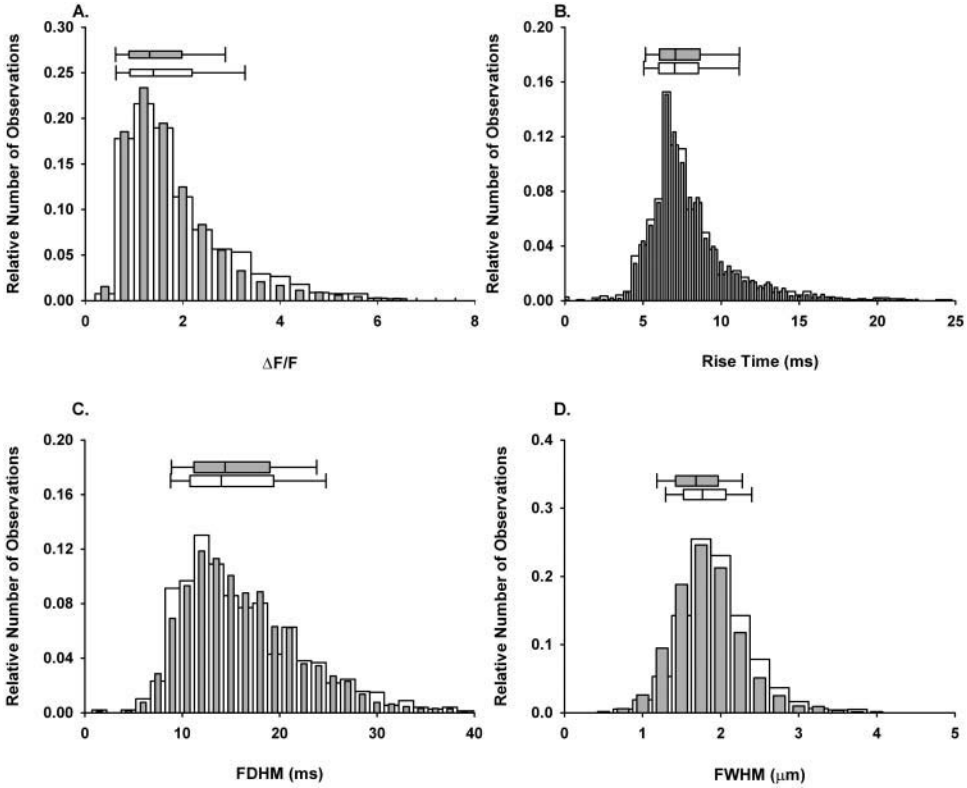

FIGURE 6 Effect of CaM on the spatiotemporal properties of spontaneous Ca^{2+} sparks. Normalized histograms of amplitudes (*A*), rise times (*B*), FDHM (*C*), and FWHM (*D*) for sham (*open bars*, $n_{events} = 1467$) or after the addition of CaM (1 μM, *closed bars*, $n_{events} = 3120$). Above each histogram is the median box plot with 25 and 75 (edge of box) and 10 and 90 (error bar cap) percentiles.

results show an increase in the frequency of spontaneous Ca^{2+} sparks at $[Ca^{2+}]_i$ of ~50–100 nM, the increase in the occurrence of spontaneous Ca^{2+} sparks is most likely a result of an interaction of Ca^{2+}-free CaM with RYR. Furthermore, it has been suggested that Ca^{2+} binding to CaM may mediate Ca^{2+} dependent closing of RYR Ca^{2+} release channels by a Ca^{2+}CaM dependent inactivation. To test whether Ca^{2+} binding to CaM is involved in the observed increase in Ca^{2+} spark frequency and/or promotes termination of spontaneous Ca^{2+} sparks we analyzed the effect of a mutant CaM (CaM_{1234}) that cannot bind Ca^{2+} under the conditions used in these studies. CaM_{1234} contains an E to Q mutation in each of the four Ca^{2+} binding sites, effectively eliminating Ca^{2+} binding under quasiphysiological conditions (Mukherjea et al., 1996; Maune et al., 1992). Fig. 9 shows that CaM_{1234} (0.5–5.0 μM) elicited a dose-dependent increase in the frequency of spontaneous Ca^{2+} sparks, with a fractional maximal increase (R) of 11.8 ± 3.7, a half-maximal activation at 0.95 ± 0.06 μM and a Hill coefficient of 3.7 ± 0.6. The similarity between the increased Ca^{2+} spark frequency between wild-type CaM and CaM_{1234} (compare Fig. 7 *A* with Fig. 9), supports the idea that Ca^{2+}-free CaM promotes the RYR channel opening that initiates the observed Ca^{2+} sparks.

If Ca^{2+} binding to CaM, and subsequent Ca^{2+}CaM dependent inactivation of Ca^{2+} release channels, played a role in the termination of Ca^{2+} release one would expect that CaM_{1234} would slow or prevent this process. These changes would prolong the open time of the channel, which would be manifested as either an increase in the amplitude or rise time of the Ca^{2+} spark, or both. Fig. 10 shows the histograms of the spatiotemporal properties along with the median box plots for the population of Ca^{2+} sparks in the presence of 1 μM of either CaM or CaM_{1234}. Compared to CaM, CaM_{1234} resulted in a small but statistically significant decrease in the amplitude (14%) and FWHM (5%),

TABLE 1 Effect of CaM on the spatiotemporal properties of spontaneous Ca^{2+} sparks

Property	Sham	CaM	CaM_{1234}
Amplitude (ΔF/F)	1.40 (0.91, 2.20)	1.32 (0.90, 1.98)*	1.13 (0.78, 1.74)*†
Rise time (ms)	7.02 (6.01, 8.54)	7.07 (6.05, 8.64)	7.12 (6.04, 8.95)
FDHM (ms)	14.00 (10.80, 19.40)	14.40 (11.20, 19.00)	14.6 (11.2, 19.8)
FWHM (μm)	1.77 (1.52, 2.07)	1.68 (1.42, 1.97)*	1.59 (1.35, 1.85)*†

Ca^{2+} spark properties were obtained from linescan images (2 ms/line) as described in Materials and Methods. The values reported are the medians with 25 and 75 percentiles in parentheses. $p < 0.05$ versus sham* or CaM†.

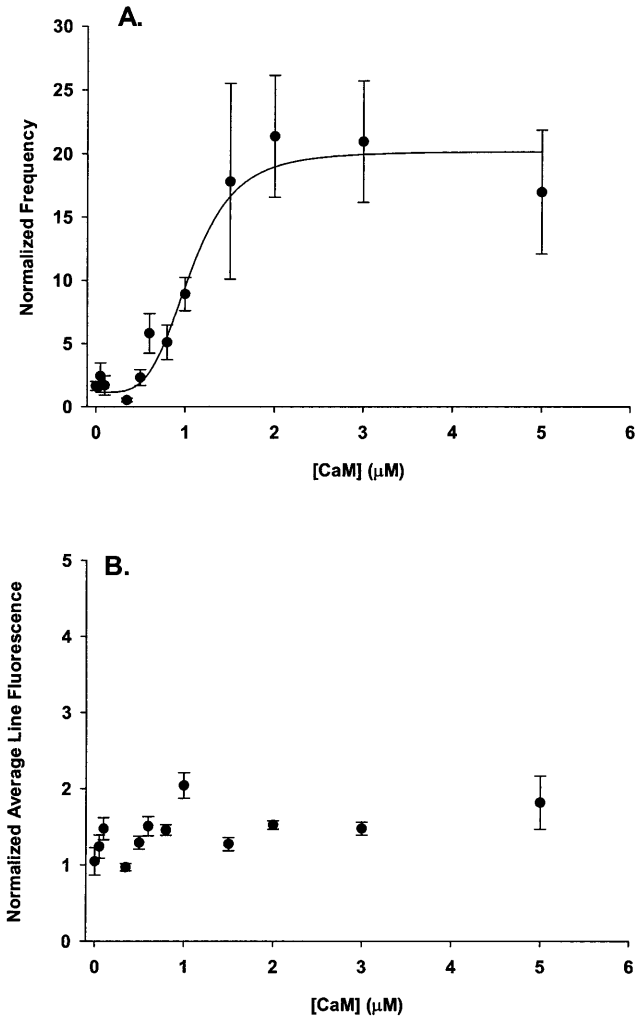

FIGURE 7 Dose-dependent effect of CaM on spontaneous Ca^{2+} spark frequency. (*A*) Frequency of spontaneous Ca^{2+} sparks before and after the addition of various concentrations of CaM (0.05–5.0 μM) at a $[Mg^{2+}]_{free}$ of 0.65 mM. To control for variability in the resting Ca^{2+} spark frequency the frequency of each fiber in the presence of the indicated CaM was normalized to the average frequency for that group of fibers prior to addition of CaM. The data for no added CaM are buffer and time controls (sham) as described in Materials and Methods. The solid line was obtained by fitting the data to Eq. 2. The fractional maximal increase in spark frequency was 17.3 ± 5.5, the EC_{50} was 1.1 ± 0.1 μM and the Hill coefficient was 4.2 ± 1.1. (*B*) Average line fluorescence of the same fibers as in *A*. All data points are presented as mean ± SE for at least four fibers at each CaM concentration.

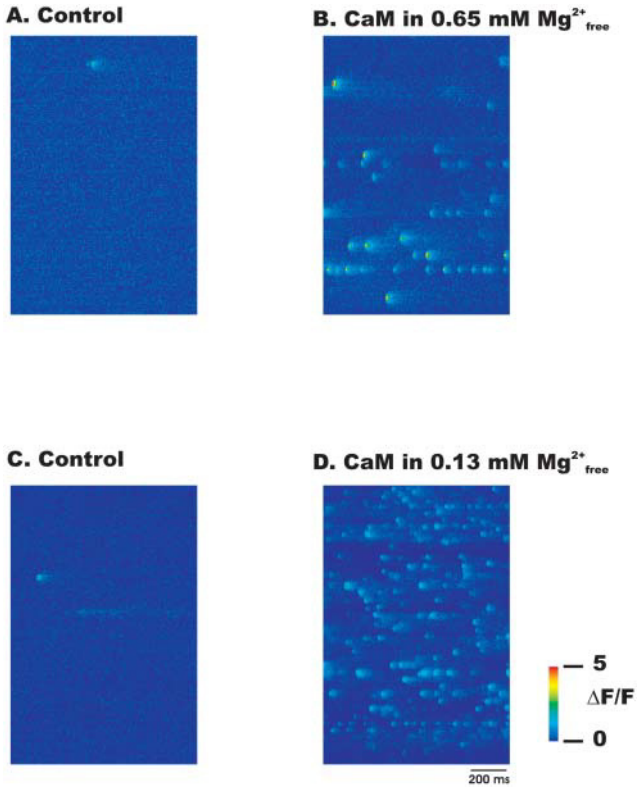

FIGURE 8 Representative linescan images showing discrete localized Ca^{2+} sparks under control condition in 0.65 mM $[Mg^{2}]_{free}$ (*A* and *C*), in 3 μM CaM and 0.65 mM $[Mg^{2+}]_{free}$ (*B*) or in 3 μM CaM and 0.13 mM $[Mg^{2+}]_{free}$ (*D*).

whereas rise time and FDHM were not significantly different (Table 1). These small changes observed in spark properties with CaM_{1234} probably do not reflect a functionally meaningful change in the opening time of the channel or the spatial spread of the released Ca^{2+}. Thus, the CaM added to the fibers in our studies dramatically increases the rate of opening of the channels underlying the initiation of Ca^{2+} sparks, but does not appear to mediate Ca^{2+}CaM dependent channel closing.

DISCUSSION

In this study we report the effects of CaM on microscopic Ca^{2+} release events (Ca^{2+} sparks) in permeabilized frog skeletal muscle. CaM is a Ca^{2+} binding protein that has previously been shown in SR vesicle and planar lipid bilayer experiments to interact with and modulate RYR1 in a Ca^{2+} dependent manner. Under low free $[Ca^{2+}]$ (<1 μM) four Ca^{2+}-free CaM molecules bind to each tetramer of RYR1 and Ca^{2+}-free CaM activates the channel (Rodney et al., 2000; Tripathy et al., 1995). Upon binding Ca^{2+}, CaM shifts toward a more N-terminal location within RYR1, with subsequent inactivation of the channel (Rodney et al., 2000, 2001). Our present findings demonstrate that recombinant wild-type CaM increases Ca^{2+} spark frequency in frog skeletal muscle fibers, with the potentiating effect of CaM saturating at low-μM concentrations. Despite a marked increase in the frequency of spontaneous Ca^{2+} sparks, CaM did not result in an appreciable change in the properties of the individual Ca^{2+} sparks. A CaM mutant that cannot bind Ca^{2+} (CaM_{1234}) caused a similar increase in Ca^{2+} spark frequency as CaM with no significant change in the properties of the individual events. These results suggest that Ca^{2+}-free CaM increases the probability of opening of the SR Ca^{2+} release channels that activate Ca^{2+} sparks. However, the

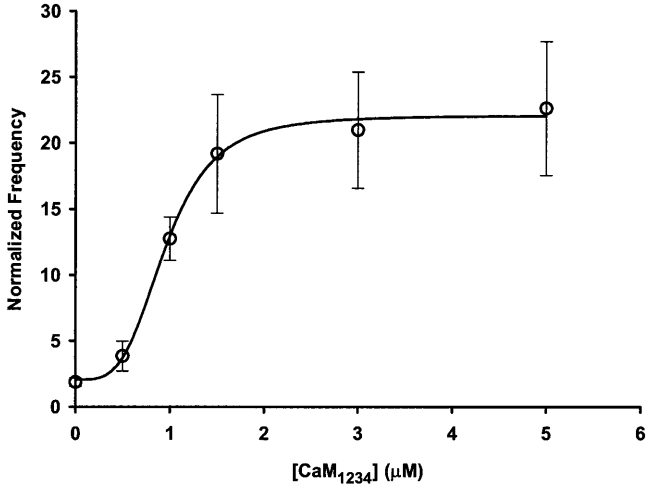

FIGURE 9 Dose-dependent effect of CaM_{1234} on spontaneous Ca^{2+} spark frequency. Frequency of spontaneous Ca^{2+} sparks before and after the addition of various concentrations of CaM_{1234} (0.5–5.0 μM) at a $[Mg^{2+}]_{free}$ of 0.65 mM. To control for variability in the resting Ca^{2+} spark frequency the frequency of each fiber in the presence of the indicated CaM_{1234} was normalized to the average frequency for that group of fibers prior to addition of CaM_{1234}. The data for no added CaM are buffer and time controls (sham) as described in Materials and Methods. The solid line was obtained by fitting the data to Eq. 2. The maximal fractional increase in spark frequency was 11.8 ± 3.7, the EC_{50} was 0.95 ± 0.06 μM and the Hill coefficient was 3.7 ± 0.6. All data points are presented as mean ± SE for at least three fibers at each CaM_{1234} concentration.

similarity of Ca^{2+} spark properties in control, CaM, and CaM_{1234} indicates that Ca^{2+} binding to exogenously added CaM does not promote closing of the channels that generate a spark.

Calmodulin increases spontaneous Ca^{2+} spark frequency

In permeabilized frog skeletal muscle CaM dramatically increased spontaneous Ca^{2+} spark frequency, indicating that CaM caused a marked increase in either the opening rate of the Ca^{2+} release channels that initiate Ca^{2+} sparks or in the probability that an open channel would trigger a Ca^{2+} spark. Immunolocalization of CaM subsequent to permeabilization shows a similar pattern and intensity as in fibers not permeabilized (Fig. 3), indicating that there is not an appreciable loss of total endogenous CaM during permeabilization. Therefore, one possible explanation for the increase in Ca^{2+} spark frequency observed here is that added exogenous CaM associates with a proportion of RYRs not bound by endogenous CaM. We hypothesize that these RYRs could be uncoupled receptors. Alternatively a majority of the endogenous CaM could be bound to sites other than RYR (Harper et al., 1980). In this case the small fraction of total endogenous CaM that is bound to RYR in intact fibers could dissociate in the permeabilized fibers without causing a detectable change in antibody staining of total endogenous CaM.

Frog skeletal muscle contains equal proportions of RYRα and RYRβ, the amphibian homologs of mammalian RYR1 and RYR3, respectively. Sequence alignment of the CaM-binding domain of RYR1 (3614–3643) shows 100% identity with RYRα (3598–3627) and 90% identity with both RYR3 (3649–3678) and RYRβ (3471–3500). Both L3624 and W3620, which are critical amino acids for Ca^{2+}-free CaM and Ca^{2+}CaM binding, respectively (Yamaguchi et al., 2001) are conserved in all isoforms. Furthermore, both RYR1 and RYR3 have been shown to be regulated by CaM (Rodney et al., 2000; Tripathy et al., 1995; Chen et al., 1997). Although RYR1(α) but not RYR3(β) can functionally couple to the DHPR (Fessenden et al., 2000), only half of the RYRα in frog skeletal muscle are believed to be coupled to DHPRs (Block et al., 1988; Flucher and Franzini-Armstrong, 1996). Recently, Felder and Franzini-Armstrong (2002) report the presence of additional foot-like structures outside the SR/T-Tubule junctional region, termed parajunctional feet. The occurrence of these parajunctional feet parallel the content of RYR3(β) in muscle fibers. Therefore, even if CaM only interacts with uncoupled RYRs, the population of RYRs responding to CaM in our studies could in principle either be RYRα, RYRβ, or both.

The dominant-negative (N+3)CaM has a higher affinity for RYR than does wild-type CaM. If (N+3)CaM exchanged for endogenous CaM remaining in permeabilized fibers one would predict a decrease in Ca^{2+} spark frequency upon the addition of (N+3)CaM. Our results in which (N + 3)CaM did not alter Ca^{2+} spark frequency could be explained by (N+3)CaM preferentially binding to RYRs that do not have endogenous CaM bound; the conditions used in these experiments may not favor (N+3)CaM displacement of a significant fraction of remaining endogenous CaM that is bound to RYR. Future experiments using higher concentrations of (N+3)CaM and/or longer incubation times may favor exchange of (N+3)CaM for endogenous CaM.

O'Connell et al. (2002) have recently reported that mutating the CaM binding site in RYR1, such that it cannot bind CaM, had little effect on voltage evoked Ca^{2+} release in primary cultured skeletal myotubes, suggesting that CaM binding to 3614–3643 on RYR1 is not necessary for voltage activated Ca^{2+} release in this system. However, the level of CaM expression and/or the fraction of RYR1 bound with CaM in these myotubes may be low, in which case the mutation of the CaM binding region within RYR1 would not influence Ca^{2+} release. Furthermore, the finding that mutating the CaM binding site in RYR1 did not significantly alter voltage activated whole cell Ca^{2+} transients does not preclude a role for CaM in all forms of SR calcium release. Our finding that CaM increased localized Ca^{2+} release events (Ca^{2+} sparks) in permeabilized skeletal muscle fibers establishes that the regulation of SR Ca^{2+} release by CaM is clearly important at the microscopic (localized Ca^{2+} release)

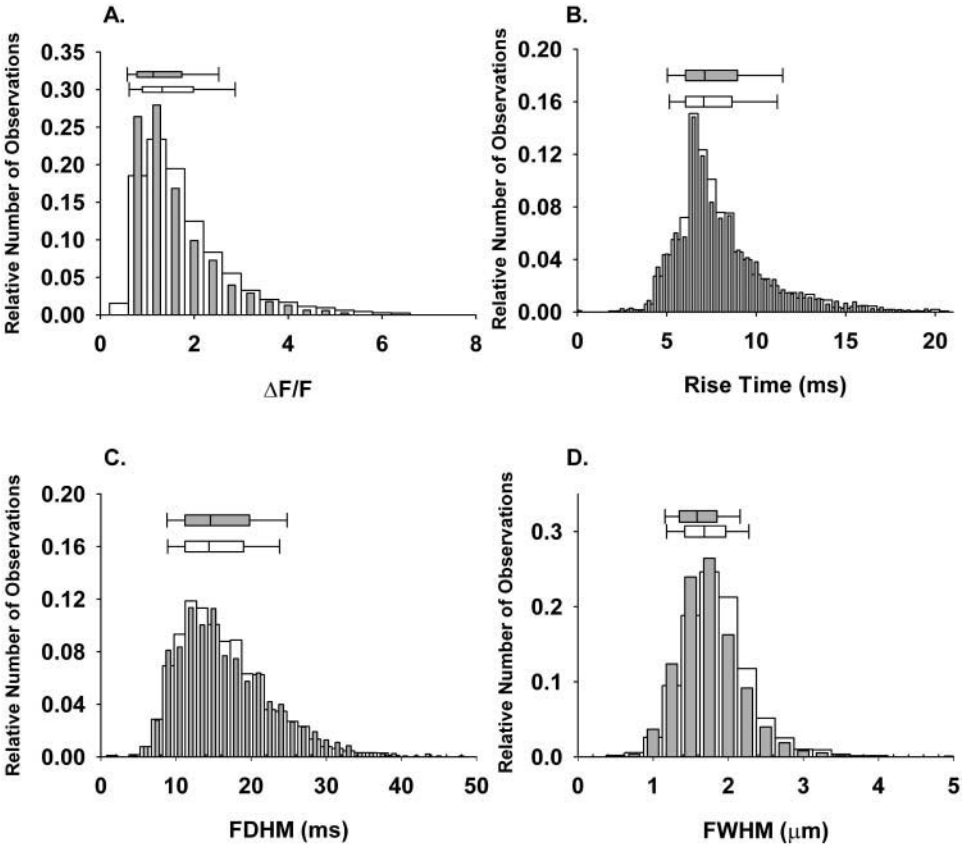

FIGURE 10 Effect of CaM_{1234} on the spatiotemporal properties of spontaneous Ca^{2+} sparks. Normalized histograms of amplitudes (*A*), rise times (*B*), FDHM (*C*), and FWHM (*D*) in the presence of either CaM (1 μM, *open bars*, $n_{events} = 3120$) or CaM_{1234} (1 μM, *closed bars*, $n_{events} = 2838$). The data for CaM are the same as those shown in Fig. 6. Above each histogram is the median box plot with 25 and 75 (edge of box), 10 and 90 (error bar cap) percentiles.

level. Recently, studies in neonatal skeletal muscle have suggested that RYR3 amplifies CICR initiated by RYR1 (Yang et al., 2001). The regulation of localized Ca^{2+} release by CaM could be of critical importance during neonatal development when the T-tubule system is not well developed, sensitizing RYR3(β) channels to Ca^{2+} and allowing for a robust Ca^{2+} signal for Ca^{2+} dependent cellular processes. Additionally, it is conceivable that CaM has an effect on voltage-induced Ca^{2+} release (and subsequent Ca^{2+} sparks) that is different from our observations reported in this study. Finally, we do not know whether some important component that might influence the CaM effect is lost upon permeabilization.

The activation of Ca^{2+} sparks by CaM was found to be concentration dependent, saturating at low μM [CaM]. To our knowledge, this is the first report in which a modulator of RYR has shown saturation in its effect on Ca^{2+} spark frequency. To our knowledge, this observation indicates that CaM binding does not directly cause or drive channel opening; otherwise the channel should go to a state of constant open as the [CaM] is increased. Furthermore, the saturation of the increased frequency of occurrence of Ca^{2+} sparks, along with our finding that the rise time of the Ca^{2+} release event is not altered by exogenous CaM, suggest that CaM binding does not directly stabilize the open state of the channel. Instead, our data are consistent with a model in which CaM binding puts RYR or a RYR macromolecular complex in a state where some or all of the steps toward channel opening are favored.

Our data showing the concentration-dependent enhancement of Ca^{2+} spark frequency gives a Hill coefficient of 4.2 (Fig. 7), suggesting a highly cooperative interaction for initiating a Ca^{2+} spark. Cooperative binding of one CaM molecule to each of at least four interacting channels, resulting in an increased probability of activation of Ca^{2+} release, could explain the observed cooperativity in the CaM dependent increase in the occurrence of Ca^{2+} sparks. Alternatively, cooperative binding of four CaM molecules to a single Ca^{2+} release channel resulting in an increase in the open probability of the channel, could also account for the observed increase in Ca^{2+} spark frequency. Attempts to fit the concentration-dependent enhancement of Ca^{2+} sparks using independent binding of one CaM molecule to each of four sites, with spark frequency being proportional to the fraction of units having all four sites occupied, was not successful. Independent binding of CaM molecules to more than four sites also did not fit the data. These observations suggest that the binding of four CaM molecules was indeed cooperative.

Studies conducted with SR vesicle preparations indicate no cooperativity in CaM binding (Moore et al., 1999; Tripathy et al., 1995) and report a Hill coefficient of only 1.3 for CaM dependent enhancement of [^{3}H]ryanodine binding,

indicating only a slight cooperativity (Tripathy et al., 1995). The difference in cooperativity reported in our studies in permeabilized skeletal muscle fibers and those in isolated SR vesicles may be due in part to a disruption of a macromolecular complex during SR vesicle preparation. Recent studies suggest that there is a Ca^{2+}-dependent interaction between the FK506 binding protein (FKBP12) and the Ca^{2+}CaM dependent protein phosphatase calcineurin (Shin et al., 2002). However, in isolated systems CaM has been shown to activate RYR1 independent of ATP (Fuentes et al., 1994; Meissner, 1986). The cooperativity observed in our experiments on skeletal muscle fibers is unlikely to be due to altered RYR phosphorylation via modulation of Ca^{2+}CaM dependent kinases or phosphatases since the ambient $[Ca^{2+}]$ was relatively low in our experimental solutions. Furthermore, a Ca^{2+}CaM inhibitory peptide, based on the Ca^{2+}CaM binding site of smooth muscle myosin light chain kinase (Torok and Trentham, 1994), did not alter the occurrence of Ca^{2+} sparks nor did it prevent the CaM-induced increase in Ca^{2+} spark frequency (data not shown), supporting the notion that Ca^{2+}CaM in not involved. Even though CaM has been reported to regulate RYR3 (Chen et al., 1997) the binding stoichiometry and the concentration dependence of CaM's activation of RyR3 have not been elucidated. Therefore, the cooperativity in enhancement of Ca^{2+} spark frequency observed here may be an important difference between CaM's regulation of RYR1(α) and RYR3(β). Currently, we cannot distinguish between these possibilities and future experiments are needed to address these differences.

Ca^{2+} binding to CaM does not decrease Ca^{2+} release during a Ca^{2+} spark

Termination of Ca^{2+} release during a spontaneous Ca^{2+} spark is a process that is not completely understood. It has been proposed that Ca^{2+} binding to the low affinity Ca^{2+} inactivation sites on RYR, due to a high local $[Ca^{2+}]$ in the immediate vicinity of an open channel, may govern channel inactivation during termination of spontaneous Ca^{2+} sparks. In vitro, Ca^{2+} binding to CaM results in a shift in CaM's binding site on RYR1 and inactivation of the channel. This CaM dependent inactivation of RYR1 does not appear due to an increase in Ca^{2+} binding to inactivation sites on RYR1 since a Ca^{2+} binding site mutant CaM was able to enhance RYR1 activity at $[Ca^{2+}]$ in which wild-type CaM inhibits the channel (Rodney et al., 2001). These previous observations suggested the hypothesis that Ca^{2+} binding to CaM could play a role in the termination of the Ca^{2+} spark.

Despite a marked increase in the frequency of spontaneous Ca^{2+} sparks in the presence of recombinant CaM in this study, the properties of the individual Ca^{2+} release events showed only very small changes. The median values for amplitude and FWHM decreased slightly after the addition of CaM. However, these changes are very small (<6%), suggesting that there is no major change in the kinetics of the Ca^{2+} spark. To further test whether Ca^{2+}CaM terminates Ca^{2+} sparks we used a mutant CaM that cannot bind Ca^{2+} at any of the four Ca^{2+} binding sites (CaM_{1234}). If the termination of the Ca^{2+} spark is due to a Ca^{2+}CaM dependent inactivation of the Ca^{2+} release channel, and if this effect occurs on the exogenous CaM molecules that increase Ca^{2+} spark frequency, then the use of CaM_{1234} should result in prolongation of Ca^{2+} release during the spark. This would be manifested as either an increase in the amplitude, a prolongation of the rise time, or both. CaM_{1234} increased Ca^{2+} spark frequency similar to CaM (Fig. 9). However, CaM_{1234} did not result in an increase in the amplitude or a prolongation of the rise time. In fact, spark amplitude decreased slightly in the presence of CaM_{1234} (Table 1). Based on these findings it is unlikely that exogenously applied CaM is playing a significant role in the termination of the Ca^{2+} spark.

In conclusion, our results indicate that in frog skeletal muscle CaM is able to increase the frequency of spontaneous Ca^{2+} sparks without altering the kinetics of the individual Ca^{2+} release events. These findings support a model in which the exogenous Ca^{2+}-free CaM primarily activates uncoupled Ca^{2+} release channels by sensitizing these channels to ''spontaneous'' activation by CICR. As the $[Ca^{2+}]_i$ increases during the release event Ca^{2+} binding to added CaM does not inactivate the Ca^{2+} release channel.

We thank Dr. Susan L. Hamilton for the generous gift of cDNA encoding the various CaMs, Chris W. Ward for assistance in computer programming and helpful discussion in preparing the manuscript, and Katalin Török for the generous gift of the MLCK peptide.

Supported by R01-NS23346 to M.F.S. Dr. Rodney received fellowship support from National Institutes of Health institutional training grant T32 NS007375 (Training Program in Cellular and Integrative Neuroscience), T32 AR07592 (Interdisciplinary Training Program in Muscle Biology) and an Individual National Research Service Award F32 NS44636.

REFERENCES

Block, B. A., T. Imagawa, K. P. Campbell, and C. Franzini-Armstrong. 1988. Structural evidence for direct interaction between the molecular components of the transverse tubule/sarcoplasmic reticulum junction in skeletal muscle. *J. Cell Biol.* 107:2587–2600.

Bukatina, A. E., B. Y. Sonkin, L. L. Alievskaya, and V. A. Yashin. 1984. Sarcomere structures in the rabbit psoas muscle as revealed by fluorescent analogs of phalloidin. *Histochemistry.* 81:301–304.

Chen, S. R. W., X. Li, K. Ebisawa, and L. Zhang. 1997. Functional characterization of the recombinant type 3 Ca^{2+} release channel (ryanodine receptor) expressed in HEK293 cells. *J. Biol. Chem.* 272: 24234–24246.

Cheng, H., W. J. Lederer, and M. B. Cannell. 1993. Calcium sparks: elementary events underlying excitation-contraction coupling in heart muscle. *Science.* 262:740–744.

Cheng, H., L. S. Song, N. Shirokova, A. Gonzalez, E. G. Lakatta, E. Rios, and M. D. Stern. 1999. Amplitude distribution of calcium sparks in confocal images: theory and studies with an automatic detection method. *Biophys. J.* 76:606–617.

Felder, E., and C. Franzini-Armstrong. 2002. Type 3 ryanodine receptors of skeletal muscle are segregated in a parajunctional position. *Proc. Natl. Acad. Sci. USA.* 99:1695–1700.

Fessenden, J. D., Y. Wang, R. A. Moore, S. R. W. Chen, P. D. Allen, and I. N. Pessah. 2000. Divergent Functional Properties of Ryanodine Receptor Types 1 and 3 Expressed in a Myogenic Cell Line. *Biophys. J.* 79:2509–2525.

Fill, M., and J. A. Copello. 2002. Ryanodine Receptor Calcium Release Channels. *Phys. Rev.* 82:893–922.

Flucher, B. E., and C. Franzini-Armstrong. 1996. Formation of junctions involved in excitation-contraction coupling in skeletal and cardiac muscle. *Proc. Natl. Acad. Sci. USA.* 93:8101–8106.

Fuentes, O., C. Valdivia, D. Vaughan, R. Coronado, and H. H. Valdivia. 1994. Calcium-dependent block of ryanodine receptor channel of swine skeletal muscle by direct binding of calmodulin. *Cell Calcium.* 15:305–316.

Gonzalez, A., W. G. Kirsch, N. Shirokova, G. Pizarro, G. Brum, I. N. Pessah, M. D. Stern, H. Cheng, and E. Rios. 2000. Involvement of multiple intracellular release channels in calcium sparks of skeletal muscle. *Proc. Natl. Acad. Sci. USA.* 97:4380–4385.

Harper, J. F., W. Y. Cheung, R. W. Wallace, H. L. Huang, S. N. Levine, and A. L. Steiner. 1980. Localization of calmodulin in rat tissues. *Proc. Natl. Acad. Sci. USA.* 77:366–370.

James, P., T. Vorherr, and E. Carafoli. 1995. Calmodulin-binding Domains: Just Two Faced or Multi-faceted? *Trends Biochem. Sci.* 20:38–42.

Klein, M. G., H. Cheng, L. F. Santana, Y. H. Jiang, W. J. Lederer, and M. F. Schneider. 1996. Two mechanisms of quantized calcium release in skeletal muscle. *Nature.* 379:455–458.

Lacampagne, A., C. W. Ward, M. G. Klein, and M. F. Schneider. 1999. Time course of individual Ca2+ sparks in frog skeletal muscle recorded at high time resolution. *J. Gen. Physiol.* 113:187–198. (Published correction appears in *J. Gen. Physiol.* 2003. 121:179.)

Lacampagne, A., M. G. Klein, and M. F. Schneider. 1998. Modulation of the frequency of spontaneous sarcoplasmic reticulum Ca^{2+} release events (Ca^{2+} sparks) by myoplasmic [Mg2+] in frog skeletal muscle. *J. Gen. Physiol.* 111:207–224.

Maune, J. F., C. B. Klee, and K. Beckingham. 1992. Ca^{2+} binding and conformational change in two series of point mutations to the individual Ca^{2+}-binding sites of calmodulin. *J. Biol. Chem.* 267:5286–5295.

Meissner, G. 1986. Evidence for a role of calmodulin in the regulation of calcium release from skeletal muscle sarcoplasmic reticulum. *Biochemistry.* 25:244–251.

Moore, C. P., G. Rodney, J. Z. Zhang, L. Santacruz-Toloza, G. Strasburg, and S. L. Hamilton. 1999. Apocalmodulin and Ca^{2+} calmodulin bind to the same region on the skeletal muscle Ca2+ release channel. *Biochemistry.* 38:8532–8537.

Mukherjea, P., J. F. Maune, and K. Beckingham. 1996. Interlobe communication in multiple calcium-binding site mutants of *Drosophila* calmodulin. *Protein Sci.* 5:468–477.

O'Connell, K. M. S., N. Yamaguchi, G. Meissner, and R. T. Dirksen. 2002. Calmodulin binding to the 3614–3643 region of RyR1 is not essential for excitation-contraction coupling in skeletal myotubes. *J. Gen. Physiol.* 120:337–347.

Ogawa, Y., T. Murayama, and N. Kurebayashi. 2002. Ryanodine receptor isoforms of non-mammalian skeletal muscle. *Front. Biosci.* 7:d1184–d1194.

Pate, P., J. Mochca-Morales, Y. Wu, J. Z. Zhang, G. G. Rodney, I. I. Serysheva, B. Y. Williams, M. E. Anderson, and S. L. Hamilton. 2000. Determinants for calmodulin binding on voltage-dependent Ca^{2+} channels. *J. Biol. Chem.* 275:39786–39792.

Richman, P. G., and C. B. Klee. 1979. Specific perturbation by Ca^{2+} of tyrosyl residue 138 of calmodulin. *J. Biol. Chem.* 254:5372–5376.

Rodney, G. G., C. P. Moore, B. Y. William, J. Z. Zhang, J. Krol, S. E. Pedersen, and S. L. Hamilton. 2001. Calcium binding to calmodulin leads to an N-terminal shift in its binding site on the ryanodine receptor. *J. Biol. Chem.* 276:2069–2074.

Rodney, G. G., B. Y. Williams, G. M. Strasburg, K. Beckingham, and S. L. Hamilton. 2000. Regulation of RYR1 activity by Ca^{2+} and calmodulin. *Biochemistry.* 39:7807–7812.

Sencer, S., R. V. L. Papineni, D. B. Halling, P. Pate, J. Krol, J. Z. Zhang, and S. L. Hamilton. 2001. Coupling of RYR1 and L-type calcium channels via calmodulin binding domains. *J. Biol. Chem.* 38237–38241.

Shin, D. W., Z. Pan, A. Bandyopadhyay, M. B. Bhat, D. H. Kim, and J. Ma. 2002. Ca^{2+}-dependent interaction between FKBP12 and calcineurin regulates activity of the Ca^{2+} release channel in skeletal muscle. *Biophys. J.* 83:2539–2549.

Shtifman, A., C. W. Ward, J. Wang, H. H. Valdivia, and M. F. Schneider. 2000. Effects of imperatoxin A on local sarcoplasmic reticulum Ca^{2+} release in frog skeletal muscle. *Biophys. J.* 79:814–827.

Shtifman, A., C. W. Ward, T. Yamamoto, J. Wang, B. Olbinski, H. H. Valdivia, N. Ikemoto, and M. F. Schneider. 2001. Interdomain interactions within ryanodine receptors regulate Ca^{2+} spark frequency in skeletal muscle. *J. Gen. Physiol.* 119:15–32.

Torok, K., and D. R. Trentham. 1994. Mechanism of 2-chloro-(epsilon-amino-Lys75)-[6-[4-(N,N-diethylamino)phenyl]-1,3,5-triazin-4-yl]calmodulin interactions with smooth muscle myosin light chain kinase and derived peptides. *Biochemistry.* 33:12807–12820.

Tripathy, A., L. Xu, G. Mann, and G. Meissner. 1995. Calmodulin activation and inhibition of skeletal muscle Ca^{2+} release channel (ryanodine receptor). *Biophys. J.* 69:106–119.

Tsuchiya, T. 1988. Passive interaction between sliding filaments in the osmotically compressed skinned muscle fibers of the frog. *Biophys. J.* 53:415–423.

Ward, C. W., A. Lacampagne, M. G. Klein, and M. F. Schneider. 1998. Ca2+ spark properties in saponin permeabilized skeletal muscle. *Biophys. J.* 72:A269.

Xiong, L. W., R. A. Newman, G. G. Rodney, O. Thomas, J. Z. Zhang, A. Persechini, M. A. Shea, and S. L. Hamilton. 2002. Lobe-dependent regulation of ryanodine receptor type 1 by calmodulin. *J. Biol. Chem.* 277:40862–40870.

Yamaguchi, N., C. Xin, and G. Meissner. 2001. Identification of apocalmodulin and Ca^{2+}-calmodulin regulatory domain in skeletal muscle Ca^{2+} release channel, ryanodine receptor. *J. Biol. Chem.* 276: 22579–22585.

Yang, D., Z. Pan, H. Takeshima, C. Wu, R. Y. Nagaraj, J. Ma, and H. Cheng. 2001. RyR3 amplifies RyR1-mediated Ca2+-induced Ca2+ release in neonatal mammalian skeletal muscle. *J. Biol. Chem.* 276: 40210–40214.